NASA/TM—2014-218346

Design and Development of Aerogel-Based Antennas for Aerospace Applications: A Final Report to the NARI Seedling

Mary Ann B. Meador and Felix A. Miranda
Glenn Research Center, Cleveland, Ohio

August 2014

NASA STI Program . . . in Profile

Since its founding, NASA has been dedicated to the advancement of aeronautics and space science. The NASA Scientific and Technical Information (STI) program plays a key part in helping NASA maintain this important role.

The NASA STI Program operates under the auspices of the Agency Chief Information Officer. It collects, organizes, provides for archiving, and disseminates NASA's STI. The NASA STI program provides access to the NASA Aeronautics and Space Database and its public interface, the NASA Technical Reports Server, thus providing one of the largest collections of aeronautical and space science STI in the world. Results are published in both non-NASA channels and by NASA in the NASA STI Report Series, which includes the following report types:

- TECHNICAL PUBLICATION. Reports of completed research or a major significant phase of research that present the results of NASA programs and include extensive data or theoretical analysis. Includes compilations of significant scientific and technical data and information deemed to be of continuing reference value. NASA counterpart of peer-reviewed formal professional papers but has less stringent limitations on manuscript length and extent of graphic presentations.

- TECHNICAL MEMORANDUM. Scientific and technical findings that are preliminary or of specialized interest, e.g., quick release reports, working papers, and bibliographies that contain minimal annotation. Does not contain extensive analysis.

- CONTRACTOR REPORT. Scientific and technical findings by NASA-sponsored contractors and grantees.

- CONFERENCE PUBLICATION. Collected papers from scientific and technical conferences, symposia, seminars, or other meetings sponsored or cosponsored by NASA.

- SPECIAL PUBLICATION. Scientific, technical, or historical information from NASA programs, projects, and missions, often concerned with subjects having substantial public interest.

- TECHNICAL TRANSLATION. English-language translations of foreign scientific and technical material pertinent to NASA's mission.

Specialized services also include creating custom thesauri, building customized databases, organizing and publishing research results.

For more information about the NASA STI program, see the following:

- Access the NASA STI program home page at *http://www.sti.nasa.gov*

- E-mail your question to *help@sti.nasa.gov*

- Fax your question to the NASA STI Information Desk at 443–757–5803

- Phone the NASA STI Information Desk at 443–757–5802

- Write to:
  STI Information Desk
  NASA Center for AeroSpace Information
  7115 Standard Drive
  Hanover, MD 21076–1320

NASA/TM—2014-218346

Design and Development of Aerogel-Based Antennas for Aerospace Applications: A Final Report to the NARI Seedling

Mary Ann B. Meador and Felix A. Miranda
Glenn Research Center, Cleveland, Ohio

National Aeronautics and
Space Administration

Glenn Research Center
Cleveland, Ohio 44135

August 2014

Acknowledgments

The authors would like to thank Ms. Sarah Wright (California Institute of Technology Student Summer Intern), Ms. Elizabeth Barrios, Ms. Anna Sandberg, Ms. Emily MacMillon (all NASA Undergraduate Student Researcher Program), and Dr. Baochau N. Nguyen (GRC RHD/Senior Scientist, Ohio Aerospace Institute) for supporting the aerogel materials fabrication used in this work. Our thanks to Dr. Fred W. Van Keuls (GRC RHA/Vantage Partners, LLC), Dr. Carl H. Mueller (GRC RHA/Qinetiq NA), Ms. Elizabeth McQuaid (GRC FTF), Mr. Nicholas Varaljay (GRC FTF), and Dr. Rafael Rodríguez-Solís (GRC Summer Faculty Fellow, University of Puerto Rico-Mayagüez) for their support in the antenna simulations, fabrication and RF characterization. We are also thankful to Professor Maggie Chen, Texas State University-San Marcos, for the fabrication of the ink-jet printed slot coupled patch antenna element investigated in this work. Finally, we want to express our gratitude to the Aerospace Research Mission Directorate (ARMD) Seedling Proposal Program for their support of this task.

Level of Review: This material has been technically reviewed by technical management.

Available from

NASA Center for Aerospace Information
7115 Standard Drive
Hanover, MD 21076–1320

National Technical Information Service
5301 Shawnee Road
Alexandria, VA 22312

Available electronically at http://www.sti.nasa.gov

Design and Development of Aerogel-Based Antennas for Aerospace Applications: A Final Report to the NARI Seedling

Mary Ann B. Meador and Felix A. Miranda
National Aeronautics and Space Administration
Glenn Research Center
Cleveland, Ohio 44135

Abstract

As highly porous solids possessing low density and low dielectric permittivity combined with good mechanical properties, polyimide (PI) aerogels offer great promise as an enabling technology for lightweight aircraft antenna systems. While they have been aggressively explored for thermal insulation, barely any effort has been made to leverage these materials for antennas or other applications that take advantage of their aforementioned attributes. In Phase I of the NARI Seedling Project, we fabricated PI aerogels with properties tailored to enable new antenna concepts with performance characteristics (wide bandwidth and high gain) and material properties (low density, environmental stability, and robustness) superior to the state of practice (SOP). We characterized electromagnetic properties, including permittivity, reflectivity, and propagation losses for the aerogels. Simple, prototype planar printed circuit patch antennas from down-selected aerogel formulations were fabricated by molding the aerogels to net shapes and by gold-metalizing the pattern onto the templates via electron beam evaporation in a clean room environment. These aerogel based antennas were benchmarked against current antenna SOP, and exhibited both broader bandwidth and comparable or higher gain performance at appreciably lower mass. Phase II focused on the success of the Phase I results pushing the PI aerogel based antenna technology further by exploring alternative antenna design (i.e., slot coupled antennas) and by examining other techniques for fabricating the antennas including ink jet printing with the goal of optimizing antenna performance and simplifying production. We also examined new aerogel formulations with better moisture and solvent resistance to survive processing conditions. In addition, we investigated more complex antenna designs including passive phased arrays such as 2×4 and 4×8 element arrays to assess the scalability of the aerogel antenna concept. Furthermore, we explored the possibility of developing these arrays in thin, flexible form to make conformable antennas.

Introduction

The design and optimization of communication system technologies in support of aerospace platforms is of paramount interest in the aviation industry, for government (e.g., NASA, Department of Defense, etc.) and the commercial sector. Among the key technologies are transmit/receive (Tx/Rx) antennas required for communications (voice, high data rate video, internet, etc.) and navigation (GPS). A typical commercial and/or military aircraft (e.g., Boeing 737) could have as many as 15 to 100 antenna systems. This large number of antennas not only adds weight to the aircraft but also increases the complexity, and challenges the structural integrity of the fuselage. The latter is exacerbated in commuter and general aviation aircraft because of more limited space for antenna placement. Therefore approaches that could reduce the mass and number of antennas in the aforementioned aircraft and any other pertinent airborne platform (e.g., long duration, high altitude platforms) without sacrificing performance are highly desired.

An innovative approach for lightweight antennas is to use aerogels which are highly porous solids with many interesting properties, including low density and low dielectric permittivity. The latter can reduce Radio Frequency (RF) losses and improve impedance matching in the antenna. In this project, we developed antennas incorporating a robust new form of polyimide aerogel developed at GRC to address

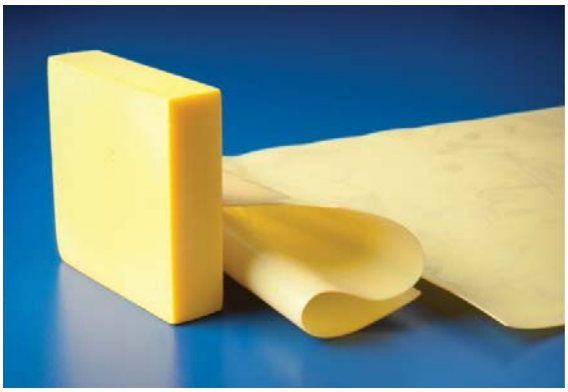

Figure 1.—Polyimide aerogels developed at GRC.

the challenges of reducing the mass and number of antennas, without sacrificing performance. The polyimide aerogels have superior mechanical strength over other types of aerogels and are easily fabricated into various forms as shown in Figure 1, making them suitable for this application. However, this project requires detailed knowledge of electromagnetic properties of the aerogels.

Use of durable aerogels enables the design of lighter, wider bandwidth, higher gain, and even conformal antennas with potential for reduction of the number of antennas in aircraft and aeronautic platforms, reduction in mass and lower cost. The level of impact of mass savings will depend on antenna aperture size. Insertion of aerogels as components of planar printed circuit antennas will enable wider operational bandwidths, reduce the number of antenna apertures required to support communication requirements, and reduce discontinuities in the aircraft fuselage, the latter being more relevant for small general aviation aircraft and unmanned air vehicles (UAV). Flexible forms of aerogel may allow conformal, drag-free “wrap-able” antennas. In addition, Earth Science remote sensing applications from LEO/GEO telecommunication satellites can also benefit from this work, due to the advantages of using porous substrates in vacuum applications (less warping and out-gassing). The mass savings from fewer and lighter antennas could allow next generation aircraft/satellite designers to include additional payload electronics to enhance flying, navigation, and surveillance capabilities, or add more fuel to extend range or time aloft. The above is consistent with the ARMD goal for advances that improve aircraft and system efficiency.

Approach and Results of Phase I

Initially, in Phase I of the project, formulations of polyimide aerogels with different backbone chemistry were fabricated in sizes suitable for dielectric characterization at multiple bandwidths. RF characterization was performed to evaluate transmission and reflection properties, and electromagnetic losses at the operational frequencies of interest for polyimide aerogels. Formulations screened in the study include polyimide aerogels cross-linked with aromatic triamine, 1,3,5-tris(aminophenoxy)benzene (TAB) and made using two different dianhydrides and mixtures of two diamines as shown in Figure 2. The diamines chosen were 4,4′-oxydianiline (ODA) and 2,2′-dimethylbenzidine (DMBZ), and the dianhydrides used were biphenyl 3,3′,4,4′-tetracarbozylic dianhydride (BPDA) and 3,3′,4,4′-benzophenone tetracarbozylic dianhydride (BTDA). The results of that study are summarized here but more details are available in Reference 1.

The dielectric constants of several formulations from this study at three frequency ranges are shown in Figure 3. As seen in the figure, BTDA formulations all have higher dielectric constant than BPDA formulations. Other trends that can be seen by modeling the X-band data using multiple linear regression analysis include a decrease in dielectric with increasing DMBZ in the formulations (Ref. 1). However, the overarching trend is that the dielectric constant decreases with decreasing density of the aerogels no matter the formulation as shown in Figure 4.

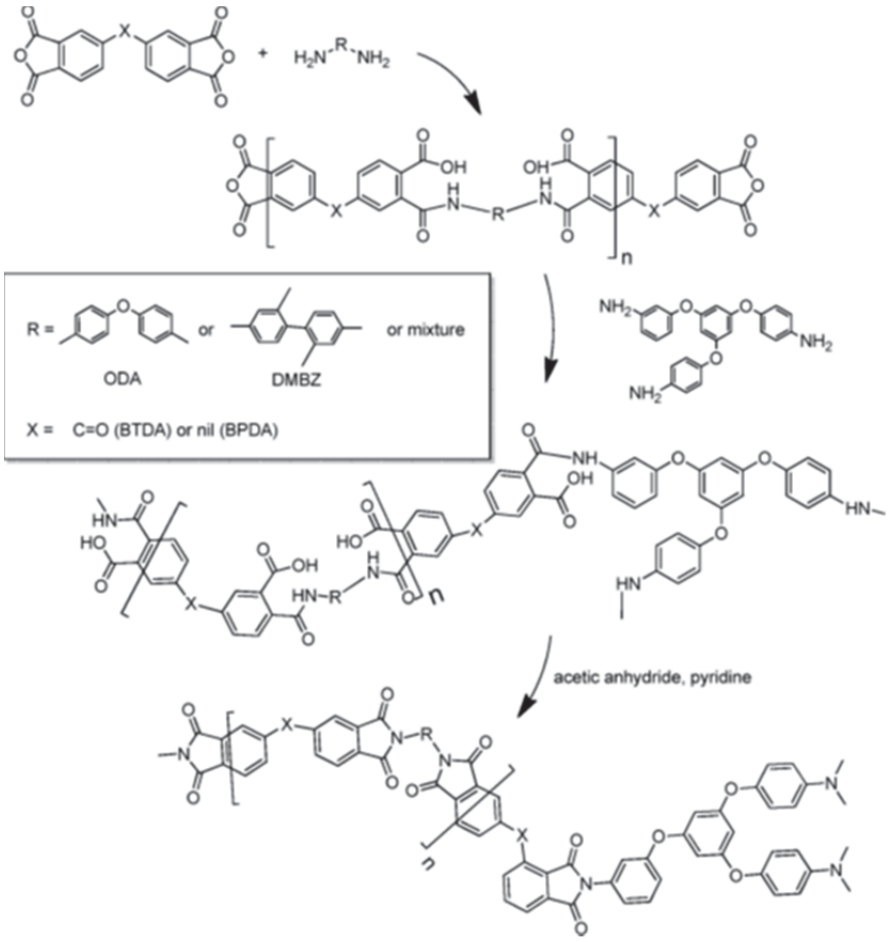

Figure 2.—Reaction scheme for synthesis of polymide aerogels from Phase I (Ref. 1).

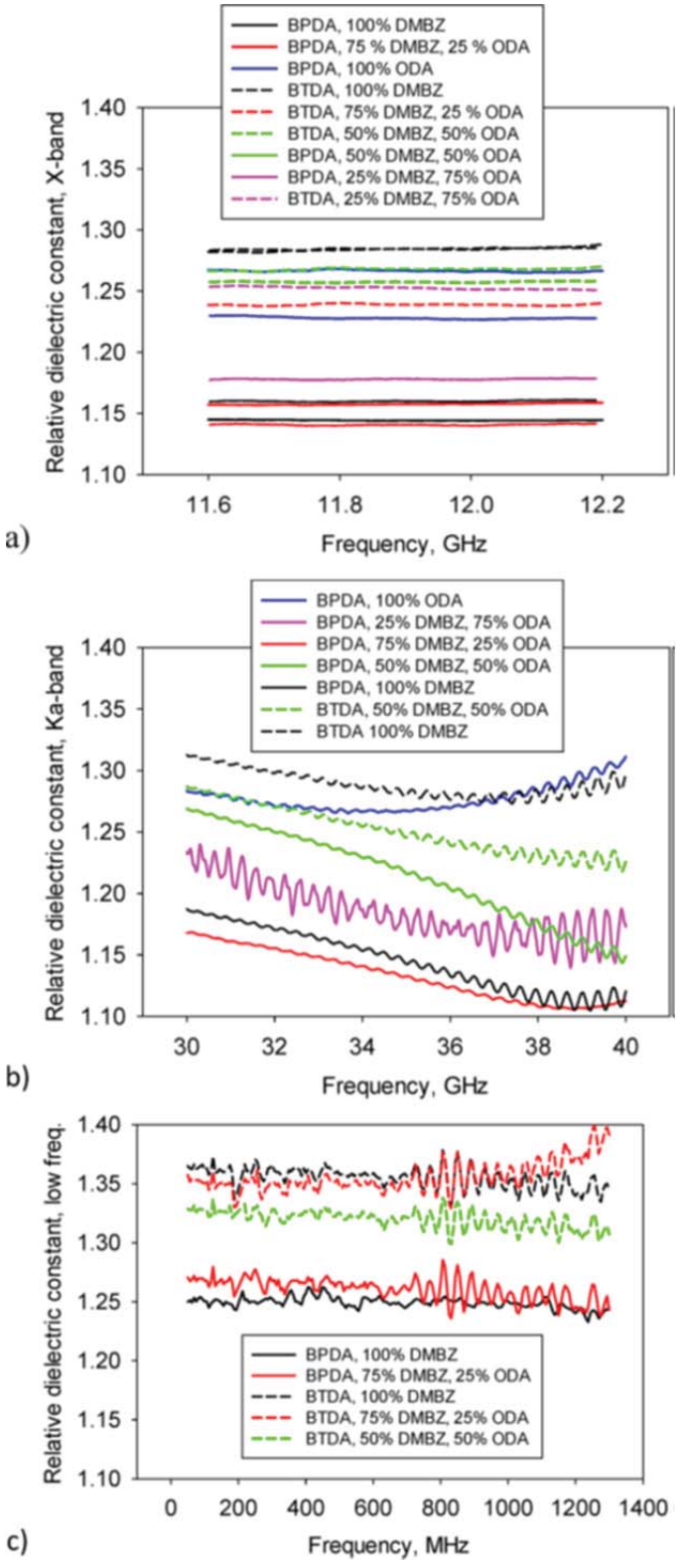

Figure 3.—Dielectric measurements at (a) X-Band, (b) Ka band, and (c) low frequency for various formulations of aerogels (average of two measurements) (Ref. 1).

In all frequency ranges measured, dielectric constants track densities of the aerogels as shown in Figure 4, while the loss tangents are all pretty similar depending on frequency range. Based on these measurements, the polyimide formulation chosen for further study was a formulation made using 100 percent DMBZ and BPDA. This formulation has the lowest dielectric constant, the best mechanical properties at the lowest density and good moisture resistance.

Larger and thinner specimens of the aerogel were then fabricated for making the patch antenna. A schematic of the printed circuit patch antenna is shown in Figure 5. Figure 6 shows actual patch antennas fabricated using three different substrates: down-selected polyimide aerogel as well as the commercially available Rogers Duroid (Rogers Corporation) 6010 and 5880. The aerogel antenna was fabricated with both the antenna and ground plane deposited with e-beam evaporated gold. Note that the aerogel substrate did warp slightly on application of the gold coating.

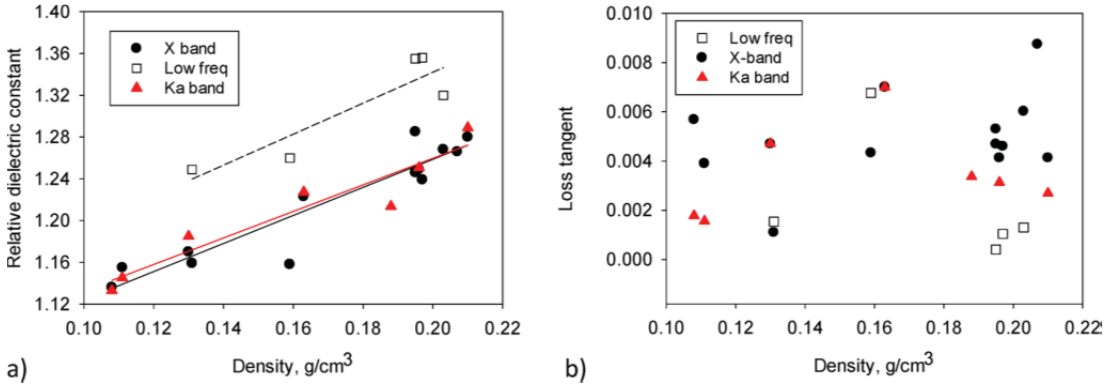

Figure 4.—Dielectric constants and loss tangents of polyimide aerogels graphed versus density (Ref. 1).

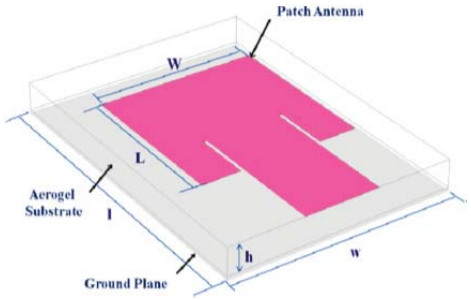

Figure 5.—Schematic of printed circuit patch antenna on an aerogel substrate (Ref. 1).

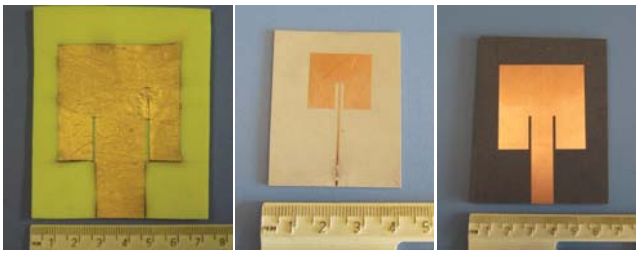

Figure 6.—Photograph of patch antenna on polyimide aerogel substrate (left), Rogers Duroid 6010 (ε_r = 10.2) (center); and Rogers Duroid 5880 (ε_r = 2.2)(right) (Ref. 1).

Figure 7 shows a plot of the measured and simulated reflection coefficient scattering parameter (S_{11}) versus frequency for the aerogel antenna compared to the Duroid antennas. Note that for all the antennas the experimental and simulated data correlate very well.

A comparison of measured bandwidth and mass of the aerogel antennas with the Duroid antennas is shown in Figure 8. It is worthwhile to highlight that the aerogel antenna exhibits both broader bandwidth and lower mass than their Duroid counterparts. In fact, the Duroid 5880 which is closer in bandwidth to the aerogel antenna has a total mass which is an order of magnitude higher. These results reinforce the potential advantages of the aerogel based antennas (ABA) antennas for aerospace applications as originally proposed.

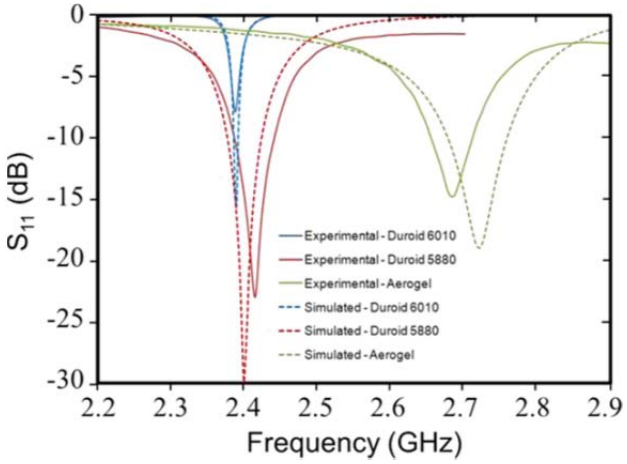

Figure 7.—Plot of S_{11} versus frequency for experimental and simulated microstrip patch antennas fabricated from polyimide aerogel (100 percent DMBZ, BPDA, and TAB) and Rogers Duroid 6010 and 5880 (Ref. 1).

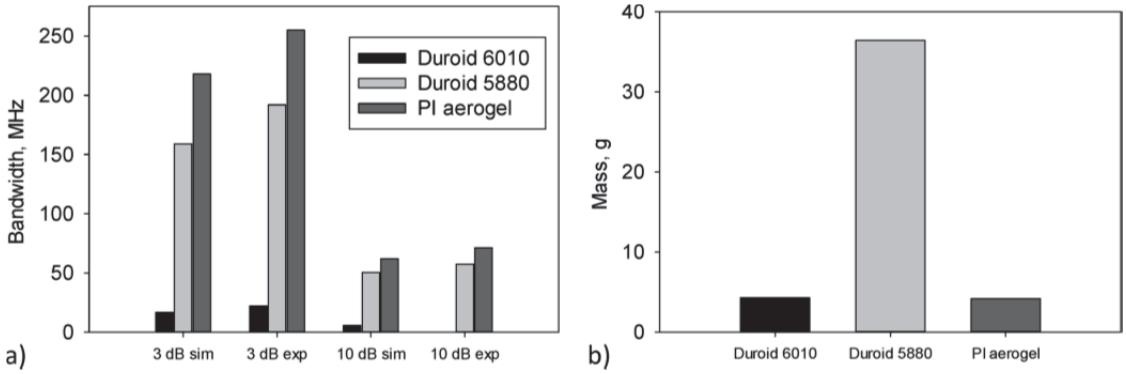

Figure 8.—Comparison of (a) bandwidth (experimental and simulated), and (b) mass of antennas fabricated from polyimide aerogel, and Rogers Duroid 6010 and 5880 (Ref. 1).

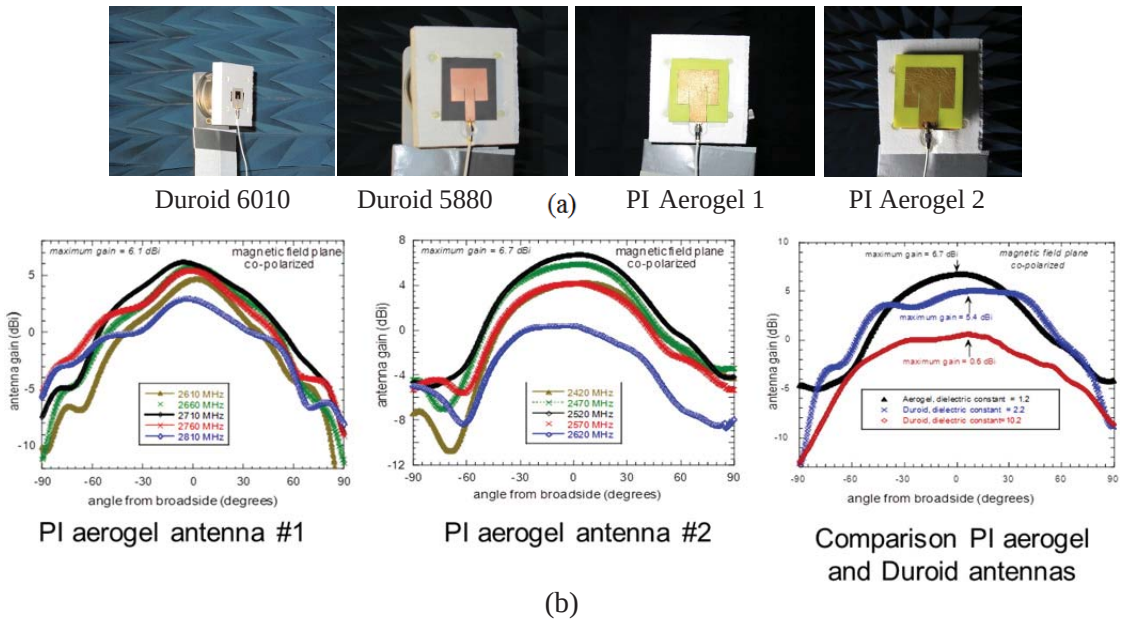

Figure 9.—(a) Printed circuit patch antennas mounted on GRC Far Field Antenna Range and (b) antenna gain versus scan angle from broadside.

Antenna gain measurements were performed at the NASA Glenn Research Center Far Field Antenna Range using the substitution method according to the IEEE Standards Test Procedures for Antennas (Ref. 3). Figure 9 shows the antennas mounted in the aforementioned range and the gain versus scan angle from broadside. The gain of the aerogel antennas surpasses that of their Duroid counterparts. Accordingly, for the printed circuit patch antenna design considered in this study, the aerogel antennas exhibit lower mass, wider bandwidth and higher gain than similar designed antennas on state of practice microwave substrate laminates.

Approach and Results of Phase II

After the results of the initial study showed that only density of the polyimide aerogels and not backbone chemistry, seemed to affect dielectric constant, it was decided to test the use of fluorinated dianhydride, 2,2-bis(3,4-dicarboxyphenyl)hexafluoropropane dianhydride (6FDA), shown in Figure 10, in place of all or part of BPDA previously used in the polyimide backbone. It was thought that the fluorinated monomers should provide greater moisture resistance and possibly lower dielectric properties since fluorinated polyimides typically have lower dielectric constants than non-fluorinated backbone structures. Because of the lower reactivity of 6FDA, catalyst for chemical imidization had to be altered and optimized. Even so, it was not possible to obtain gels from 100 percent 6FDA. A study was performed to optimize the effect of 6FDA concentration from 0 to 50 percent of total dianhydride, oligomer length (n) from 10 to 30 repeat units, and total solids concentration from 7 to 10 wt% on properties of the aerogels. The results are summarized herein but more details of the study are available in Reference 2.

Not surprisingly, reducing total solids concentration in the initial solution for gelation led to lower density aerogels as seen in Figure 11 (left). Increasing amount of 6FDA also led to lower density due to a decrease in the shrinkage that occurred during processing. As a measure of mechanical integrity, the compressive properties of the formulations were also evaluated. Figure 11 (right) shows the empirical model for modulus from compression, indicating the modulus decreases with decreasing solids concentration and increasing 6FDA fraction. Nevertheless, even the lowest modulus samples had modulus greater than 3 to 4 MPa.

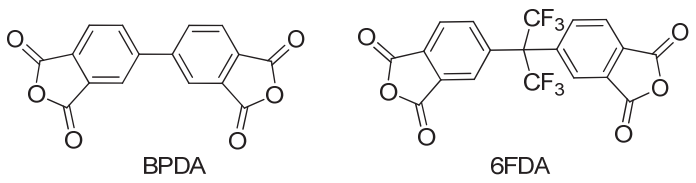

Figure 10.—Dianhydrides used in study.

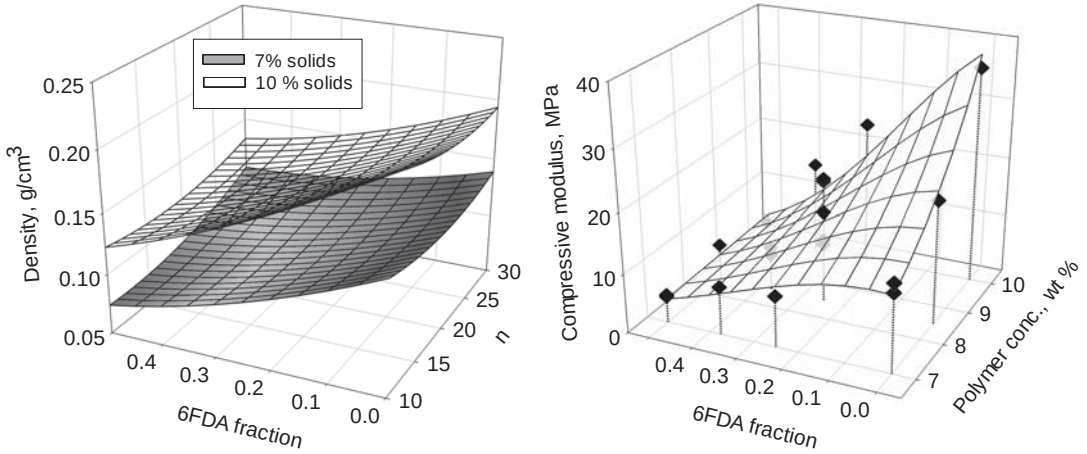

Figure 11.—Effect of variables on density (left) and modulus (right) (Ref. 2).

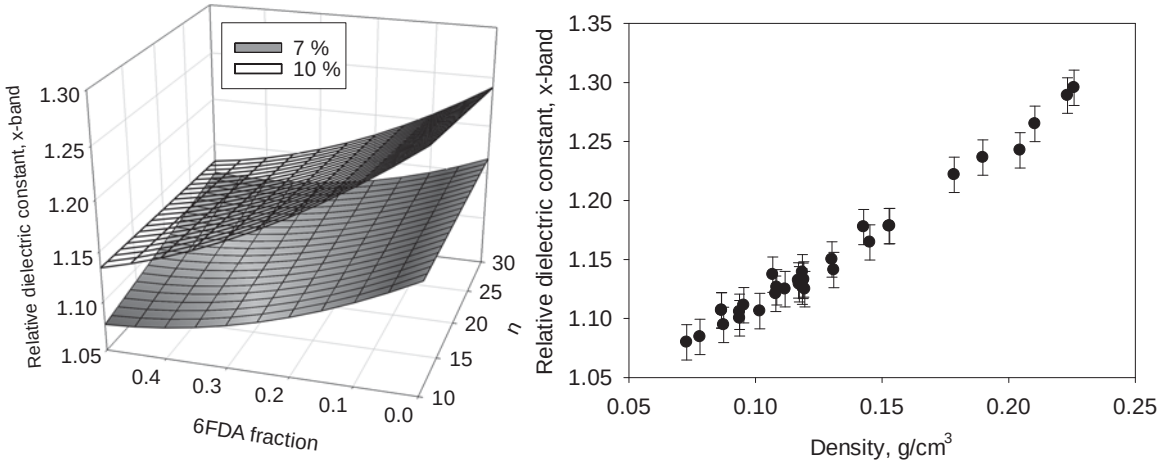

Figure 12.—Effect of (left) 6FDA concentration, n and solids content on relative dielectric constant, and (right) relative dielectric constant plotted versus density (Ref. 2).

The empirical model for relative dielectric constant of the PI aerogels in the experimental design is shown in Figure 12 (left). Dielectric constants ranged from 1.25 down to 1.08 for the lowest density samples. As seen in the graph, dielectric constant decreases with increasing 6FDA concentration and decreasing solids content. Interestingly, the empirical models for density and relative dielectric constant are nearly identical. This suggests that the dielectric properties are again dominated by density of the aerogel, regardless of the amount of fluorine content. Indeed, Figure 12 (right) shows dielectric constant plotted versus density, revealing a strong linear relationship independent of the amount of 6FDA used in the aerogels. Since the 6FDA containing aerogels tend to be less robust, the previous down selected formulation studied in Phase I with DMBZ and BPDA is still the better candidate for antennas. These results show that it too can be made with lower density by reducing solids concentration and it is expected that lower relative dielectric constants and better mechanical properties would be the result.

Antenna Fabrication and Testing in Phase II

The typical photolithography process requires exposing the PI aerogels to a series of solutions (both aqueous and organic). Because of the highly porous nature of the aerogels (90 to 97 percent porosity), it has not yet been possible to avoid the absorption of these solutions into the aerogel during the process. As an alternative, we have examined the potential of using ink jet printing of the antenna patterns on the aerogel. While initial attempts resulted in a poorly printed patch with bleeding around the edges, refined techniques resulted in a good quality patch, shown in Figure 13. This antenna exhibited gain values of 4.5 and 7.7 dBi at 4.4 and 5.0 GHz, respectively, which are comparable to those obtained with the e-beam evaporation approach. Hence, this technique could offer a viable alternative for the fabrication of antennas on aerogels or other substrates sensitive to the processing steps of standard chemical photolithography techniques.

While there are a variety of approaches to develop phased array antennas, for the purpose of this study we have selected the slot coupled design approach (Ref. 4). In general, the slot coupled approach facilitates the integration of beam shaping elements such as phase shifters and attenuators as well as power amplifiers (i.e., low noise for receive and high gain for transmit) into the antenna feed network. These components are essential for electronically steerable adaptively controlled antennas. Accordingly, we have selected the slot coupled approach to demonstrate aerogel-based phased array antennas. Figure 14 shows a picture of a 2×4 phased array antenna on a PI aerogel substrate. The gold printed circuit patches of the phased array were deposited using e-beam evaporation.

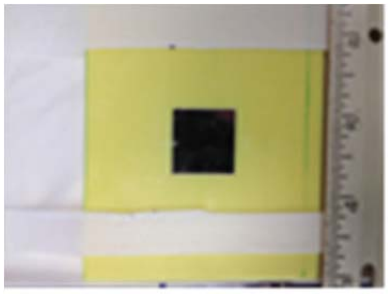

Figure 13.—Ink jet printed slot coupled patch antenna using an aerogel substrate.

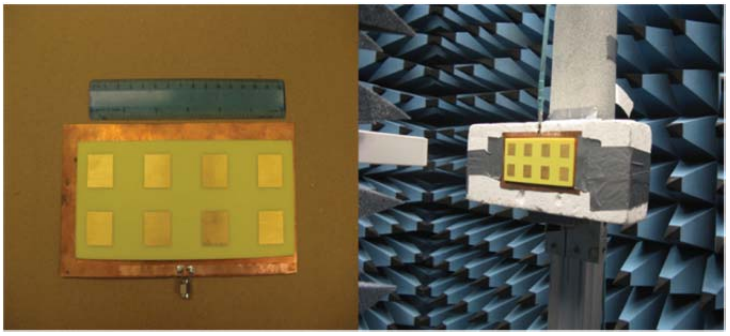

Figure 14.—E-beam evaporated 2×4 slot coupled aerogel antenna array with feed network (left); array under test at GRC's Cylindrical Near Field Antenna Range Facility (right).

Figure 15 shows the experimental and simulated H-plane and the E-plane gain data for this array at 5.0 GHz. The experimental and simulated results are in close agreement, indicating that this configuration can be scaled to larger arrays. As shown in Figure 16, a comparison of the performance of 2×4 phased arrays fabricated on aerogel and Duroid 5880 (ε_r = 2.2) substrates shows that the aerogel antenna gain is more than 1 dB higher than its Duroid counterpart (17.6 versus 16.3, respectively). Also, the mass savings of the aerogel array are substantial as shown in Table I.

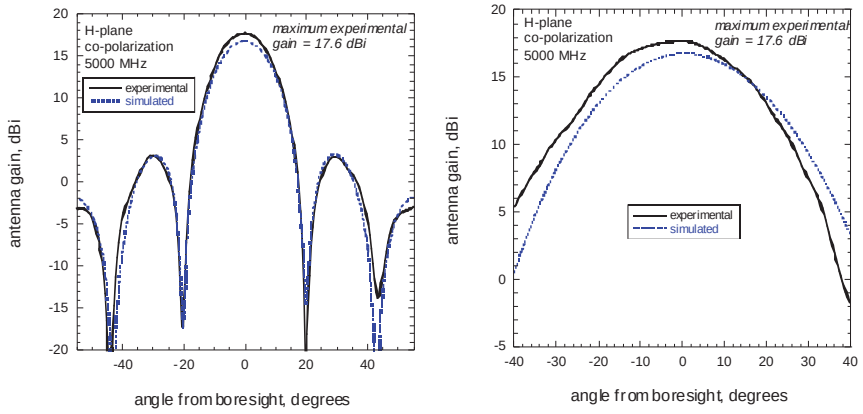

Figure 15.—Gain versus angle from bore sight for a 4×2 slot coupled aerogel antenna array. Aperture size is 15.3×5.8 cm.

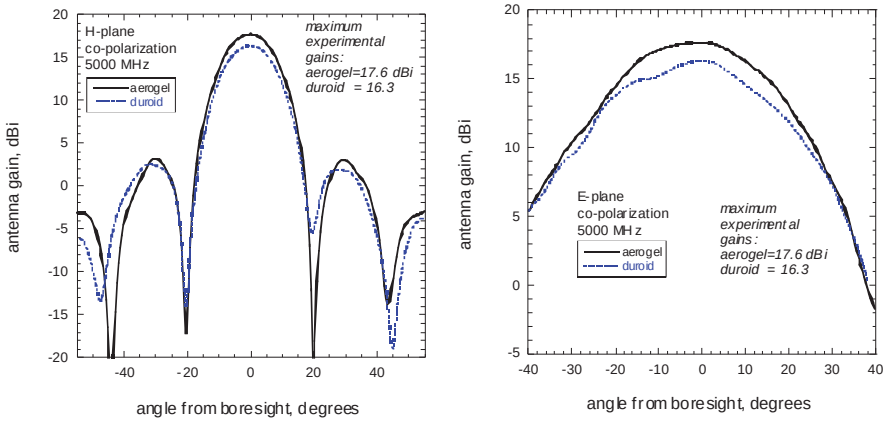

Figure 16.—Comparison of gain versus angle from bore sight for 2×4 slot coupled aerogel and Duroid (5880) arrays.

TABLE I.—MASS COMPARISON BETWEEN 2×4 AEROGEL ANTENNA AND ITS DUROID COUNTERPART

Item	Aerogel	Duroid
Radiator tile only	5.8 g (3.68 mm thick)	88.1 g (3.18 mm thick)
Feed network and ground plane (i.e., 10 mil) Duroid with copper metallization)	13.9 g	14.4 g
SMA connector weight	3.9 g (male)	1.3 g (female)
Total antenna weight	23.6 g	103.8 g

To further demonstrate the scalability of the aerogel phased arrays, a 32 element phased array made of four 2×4 aerogel tiles was fabricated. Figure 17 shows the array mounted for testing in GRC's Cylindrical Near Field Antenna Range.

Figure 18 shows the experimental and modeled H-plane and the E-plane gain for this array at 5.0 GHz. The measured gain is consistent with a uniformly illuminated aperture. As shown in Figure 19, the aerogel antennas surpass the Duroid counterpart in sustained gain over bandwidth and aperture efficiency.

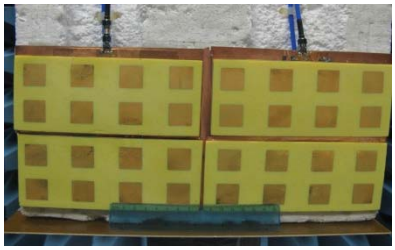

Figure 17.—E-beam evaporated 32 element slot coupled aerogel antenna comprised of four 2×4 element arrays.

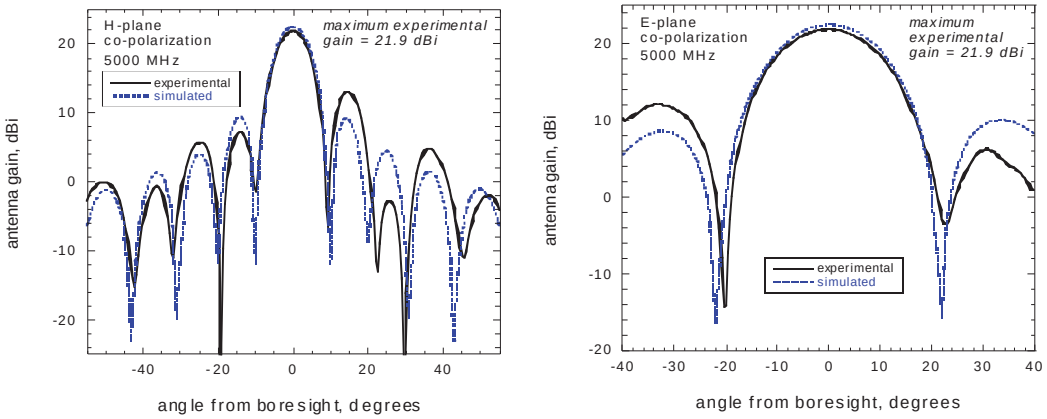

Figure 18.—Gain versus angle from boresight for a 32 element array. Total aperture size is 32.9×13.9 cm.

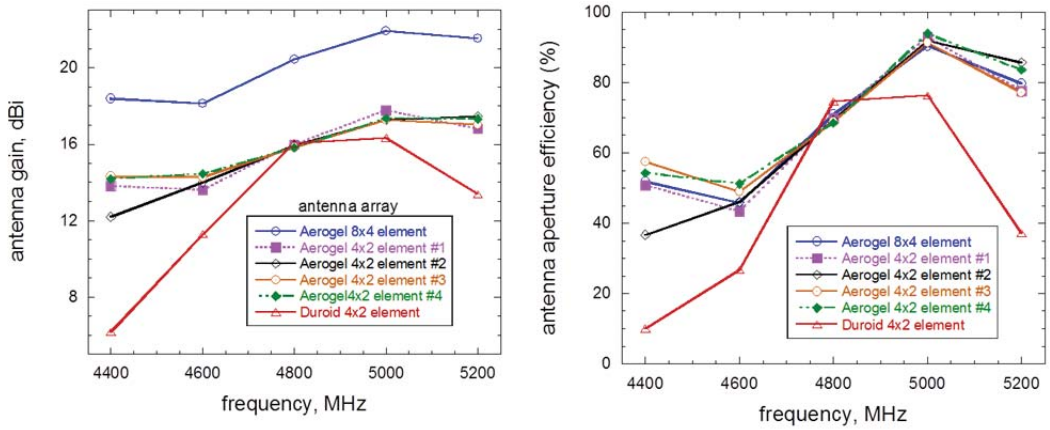

Figure 19.—Antenna gain and aperture efficiency for aerogel and Duroid antenna arrays.

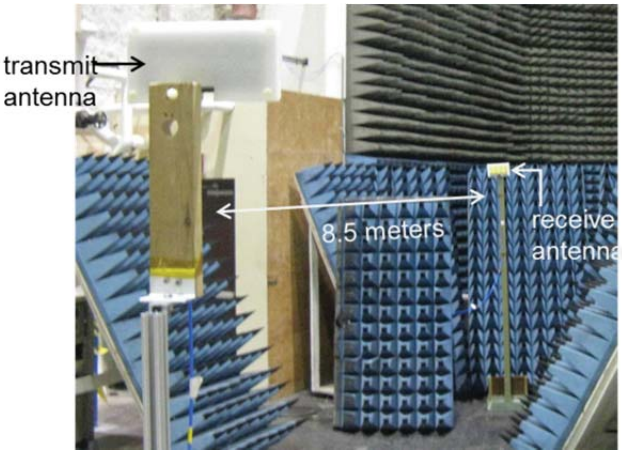

Figure 20.—Experimental set-up for EVM measurements.

To validate the usage of the aerogel phased array antennas for practical applications, a terrestrial line-of-sight (LOS) experiment was performed to investigate the suitability of the antennas to support digital communication links. The test was performed using typical modulation schemes such as Quadrature Phase Shift Keying (QPSK) and π/4-Differential Quadrature Phase Shift Keying (π/4-DQPSK). The integrity of the link was evaluated by performing Error Vector Magnitude (EVM) measurements which provide information on the extent to which experimental parameters associated with the quality of the link values deviate from reference link values. The experimental set-up for the EVM consisted of two identical 2×4 aerogel phased array antennas, one used as the transmit antenna and the other as the receive antenna, the antennas were separated by a distance of 8.5 m as shown in Figure 20. The aforementioned separation satisfies the $2D^2/\lambda$ far field criteria, where D is the maximum antenna aperture dimension and λ is the wavelength corresponding to the design frequency of the phased array. For the case under consideration D-16.1 cm, λ = 6.0 cm and $2D^2/\lambda$ = 0.864 m.

Figure 21 shows constellation graphs summarizing the performance of the 2×4 aerogel phased array antenna in the terrestrial link experiment using the aforementioned modulation schemes. The experiment was performed at a carrier frequency = 5.0 GHz; symbol rate = 7 Msps; and data rate = 14 Mbps. Also to overcome the instrumentation limitations posed by the spectrum analyzer used in this test an Avantek amplifier (AWT-6053) was placed between Rx antenna and spectrum analyzer.

Note that as the transmitted power decreases, the power received at the aerogel antenna decreases, the EVM increases and the signal-to-noise ratio (SNR) decreases. However, even at the lowest transmitted and received power levels for each of the modulation schemes, the constellation of points is still discernible indicating a viable digital communication link. The EVM measurements provide close approximation of signal to noise demodulated signal from which the bit-error-rate of the signal can be calculated. Figure 22 shows plots of EVM and SNR versus for transmitted power for the aerogel phased array at 5.0 GHz. It is worthwhile to mention that when performing EVM of the phased array 4.6 GHz and 5.4 GHz (i.e., ±0.4 GHz away from the optimal operational frequency of the antenna) the antennas maintained communications links with approximately 2.0 dB loss relative to the performance at 5.0 GHz. These results are very encouraging not only for communications but also for radar applications where the wide operational frequency range would be very useful.

Carrier frequency = 5.0 GHz; Symbol rate = 7 Msps; data rate = 14 Mbps; Avantek amplifier (AWT-6053) between Rx antenna and spectrum analyzer. Small signal gain = 27 dB; Noise figure ~4 dB

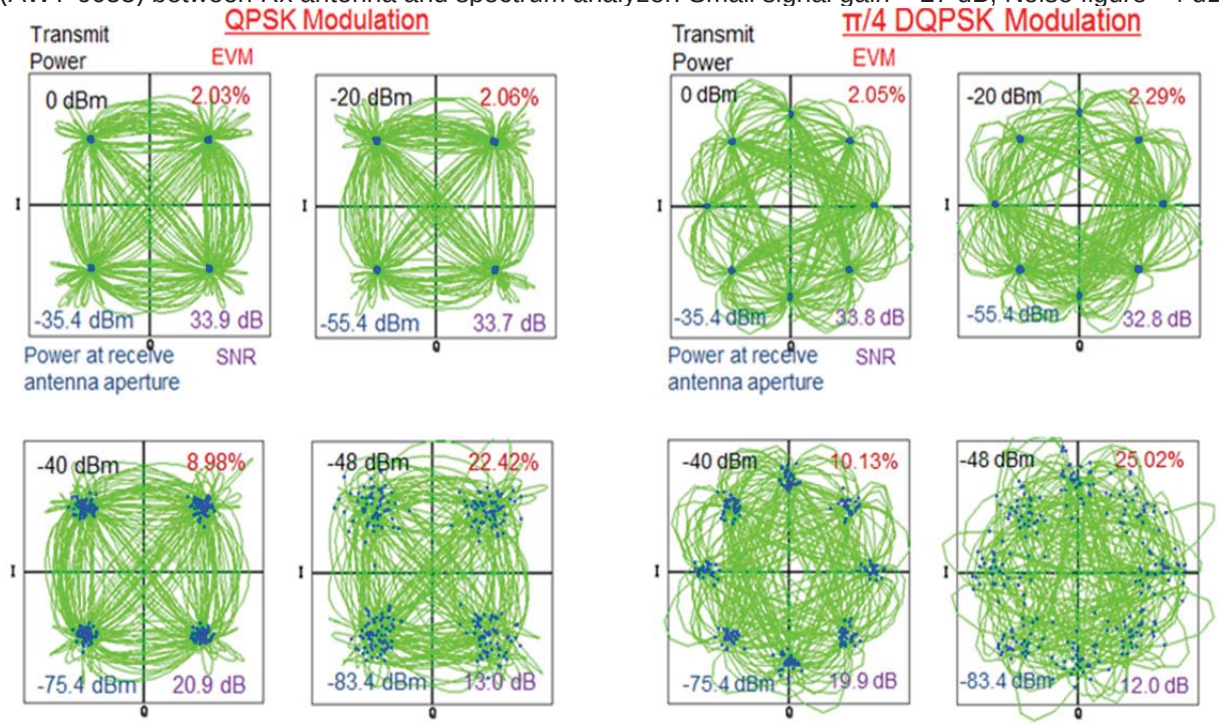

Figure 21.—Verification of antenna performance in the terrestrial link.

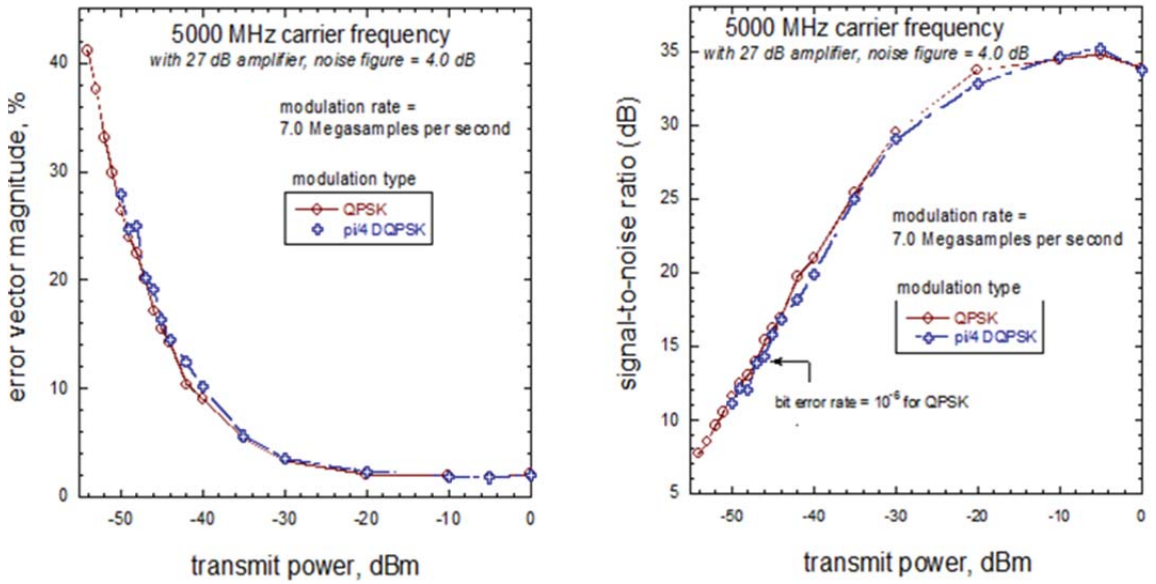

Figure 22.—EVM and SNR versus transmitted power at 5.0 GHz for the aerogel antennas.

Based on the results discussed above we also explored the possible data rates that could be enabled using the 2×4 aerogel phased array antennas in several relevant communication link scenarios such as commercial aircraft to ground, unmanned air vehicles (UAV) to ground, and cubesats to ground as shown in Figure 23. For these scenarios we considered the following: transmit and received 2×4 element aerogel phased array antennas at 5.0 GHz and with a gain of 15.6 dBi; transmit power = 2 W; receiver noise figure = 4 dB; QPSK modulation scheme; signal-to-noise ratio ≥ 14 dB; bit-error-rate (BER) ≤ 10^{-6}; no coding gain; and receiver implementation losses = 3 dB. Table II shows the data rate results when the aforementioned vehicles are 10° above the horizon (i.e., close to worst case scenario regarding free space losses). When the vehicles are directly overhead the free space losses are reduced by 7.5 dB and therefore the allowable date rates are 5.7 times higher than when the vehicle is near the horizon. Note that the date rates shown are enough to support voice and data (cubesat to ground case) and voice, data and video (UAV and commercial aircraft cases), which demonstrate the suitability of the aerogel phased array antennas to address communications requirements in these and similar platforms.

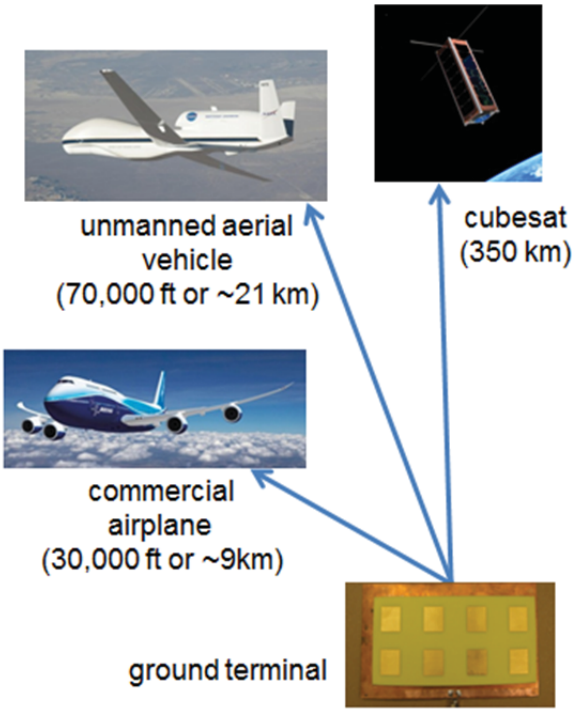

Figure 23.—Different aerospace link scenarios that could be supported by aerogel antennas. The indicated distances correspond to typical elevations when the vehicles are right overhead; i.e., at zenith.

TABLE II.—DATA RATES FOR SEVERAL AEROSPACE VEHICLES FOR ELEVATIONS 10° ABOVE THE HORIZON

Link	Maximum link distance (km)	Data rate supported
Cubesat-to-ground	2000	38 kb/s
UAV-to-ground	120	10 Mb/s
Commercial airplane-to-ground	51	58 Mb/s

Major Findings and Conclusions

The use of novel aerogel materials as substrates for radio frequency (RF) antennas has been investigated. Optimized aerogel formulations led to lower dielectric properties, better moisture/solvent resistance, and better mechanical properties. We have demonstrated the feasibility of fabricating printed circuit antennas on optimized Polyimide aerogel materials either by e-beam evaporation or ink-jet printed techniques. The performance of single-patch and phased array aerogel antennas was demonstrated with both configurations exhibiting notable advantages in mass, bandwidth, and gain over typically used microwave substrate laminates (e.g., Duroid). The aerogel antennas were demonstrated both in thick as well as thin substrates, suggesting that the attributes of PI aerogels could be maximally exploited at S- or C-band frequencies where the large physical dimensions of the antennas offer the opportunity for tailoring the array parameters (i.e., radiator size, substrate thickness, etc.) to provide optimal gain, broad bandwidth and low mass as compared to typically used microwave laminate substrates. Higher frequencies aerogel antennas could be suitable for aerospace applications requiring low profile for drag reduction and that could benefit from conformal, low profile, and reduce complexity in design offered by the aerogel antennas studied in this work. Finally, demonstration of digital communication links using common modulation schemes (e.g., QPSK and $\pi/4$-DQPSK) that could be used to support voice, data and video communication links in a variety of aerospace platforms such as UAV, commercial aircraft, and cubesats.

References

1. Meador M.A.B., Wright S., Sandberg A., Nguyen B.N., Van Keuls F.W., Mueller C H, Rodríguez-Solís R., and Miranda F.A. “Low Dielectric Polyimide Aerogels As Substrates for Lightweight Patch Antennas,” ACS Applied Materials and Interfaces, 4: 6346−6353, 2012.
2. Meador M.A.B., McMillon E, Sandberg A., Barrios E., Wilmoth N.G., Mueller C.H., and Miranda F.A. “Dielectric and Other Properties of Polyimide Aerogels Containing Fluorinated Blocks,” ACS Applied Materials and Interfaces, 6: ASAP, 2014.
3. “IEEE Standard Test Procedures for Antennas,” ANSI/IEEE Std 149−1779, 1979.
4. “Microstrip Antennas,” Chapter 14, in “Antenna Theory; Analysis and Design,” 2nd Ed., by Constantine A. Balanis, (John Wiley & Sons, Inc. 1997).